Cell. Mol. Life Sci. (2010) 67:3345–3354
DOI 10.1007/s00018-010-0386-7

Cellular and Molecular Life Sciences

RESEARCH ARTICLE

Discrimination between alternate membrane protein topologies in living cells using GFP/YFP tagging and pH exchange

Beatriz Domingo · María Gasset · Mario Durán-Prado · Justo P. Castaño · Antonio Serrano · Thierry Fischer · Juan Llopis

Received: 1 March 2010 / Revised: 30 March 2010 / Accepted: 22 April 2010 / Published online: 8 May 2010

Abstract Membrane protein function is determined by the relative organization of the protein domains with respect to the membrane. We have experimentally verified the topology of a protein with diverse orientations arising from a single primary sequence (the cellular prion protein, PrP^C), a novel somatostatin truncated receptor, and the Golgi-associated protein $GPBP_{91}$. Tagging with fluorescent proteins (FP) allows location of their expression at the plasma membrane or at endomembranes, but does not inform about their orientation. Exploiting the pH dependency of some FPs, we developed a pH exchange assay in which extracellularly exposed FPs are quenched by application of low pH buffer. We constructed standards to demonstrate and calibrate the assay, and the method was adapted for acidic organelle membrane proteins. This method can serve as a proof of concept, experimentally confirming and/or discriminating in living cells among theoretical topology predictions, providing the proportion of inside/outside orientation for proteins with multiple forms.

Keywords Membrane protein topology · Somatostatin receptor · Prion protein · Goodpasture antigen-binding protein (GPBP) · Fluorescent proteins · GFP

Abbreviations

TM	Transmembrane
ER	Endoplasmic reticulum
PM	Plasma membrane
FP	Fluorescent protein
GFP	Green fluorescent protein
YFP	Yellow fluorescent protein
GPCR	G protein-coupled receptor

Electronic supplementary material The online version of this article (doi:10.1007/s00018-010-0386-7) contains supplementary material, which is available to authorized users.

B. Domingo · J. Llopis (✉)
Centro Regional de Investigaciones Biomédicas y Facultad de Medicina, Universidad de Castilla-La Mancha,
02006 Albacete, Spain
e-mail: juan.llopis@uclm.es

M. Gasset
Instituto de Química-Física Rocasolano, CSIC,
Serrano 119, 28006 Madrid, Spain

M. Durán-Prado
Instituto de Parasitología y Biomedicina López-Neyra,
CSIC, 18100 Granada, Spain

J. P. Castaño
Departamento de Biología Celular, Fisiología e Inmunología,
Universidad de Córdoba, Edificio Severo Ochoa, Planta 3.
Campus de Rabanales, Córdoba, Spain

J. P. Castaño
Instituto Maimónides de Investigación
Biomédica de Córdoba (IMIBIC), Córdoba, Spain

J. P. Castaño
CIBER Fisiopatología de la Obesidad y
Nutrición (CIBERobn 06/03), Córdoba, Spain

A. Serrano
Hospital 12 de Octubre, 28041 Madrid, Spain

T. Fischer
Centro Nacional de Biotecnología,
CSIC, 28049 Madrid, Spain

sst	Somatostatin receptor
PrP	Prion protein
GPBP	Goodpasture antigen-binding protein
HBSS	Hanks' balanced salt solution
PEA	pH exchange assay
pH_o	Extracellular pH
pH_i	Intracellular pH
ROI	Region of interest
GPI	Glycosylphosphatidylinositol

Introduction

Membrane proteins, both bound and integrated, participate in essential cell processes such as adhesion, signaling and transport. Although membrane proteins represent up to one-third of all encoded proteins in eukaryotic cells, only a small percentage of their three-dimensional structures have been elucidated [1]. Identification of both the mode of interaction with the membrane and the relative orientation of N- and C-termini are often the first steps toward understanding membrane protein structure and function. Computational approaches are used to determine membrane protein orientation, but often provide several alternative solutions or may even bias the outcome [2, 3]. Experimental approaches are thus mandatory to elucidate unequivocally the precise structure and topology of these proteins.

Processes such as splicing, translation and translocation modulate the gain and loss of signals as well as membrane sidedness of the polypeptide chains, generating variants, isoforms and conformers that expand the functional repertoire, but also give rise to novel routes of disease. This is the case for a number of truncated somatostatin and cortistatin receptors recently reported in normal and tumor tissues, which are thus targets for drug design [4–6]. These GPCR variants lack a variable number of the typical seven-transmembrane (TM) domains, often have changes in the orientation of the N-termini, but mainly of the C-terminal tail, not easily predictable using bioinformatic tools; they are nevertheless functional in mediating signal transduction [7]. Alternative splicing of human somatostatin receptor 5 (sst5) mRNA yields a short form with three or four possible transmembrane domains, as predicted by computer algorithms (termed preliminary sst5c). Likewise, a non-canonical translation start of the protein kinase GPBP yields the $GPBP_{91}$ isoform, which is Golgi-associated [8]. Finally, a termination in chain transfer during translocation is responsible for the biogenesis of NtmPrP, a transmembrane form of the cellular prion protein (PrP^C), which has unknown metabolic properties [9–12]. Elucidation of the in/out (lumen/cytosol) membrane orientation of these three proteins would require a specific experimental approach. Here we devised such an approach by combining tagging of the protein of interest with a FP label and a pH exchange assay (PEA).

Several methods have been reported to determine protein topology with FP labels. Based on the accessibility of GFP-tagged proteins to protease digestion, a fluorescence protease protection assay was developed to indicate their orientation on the PM, or after cell membrane permeabilization by digitonin, to resolve membrane topology in intracellular organelles [13]. The bimolecular fluorescence complementation (split YFP) method requires expression of two non-fluorescent YFP fragments [14]. In addition, a ratiometric redox-based assay was recently described, in which a redox-reactive GFP reports the oxidizing state of the endoplasmic reticulum (ER) when tag orientation is lumenal and a reducing potential when it is cytoplasmic [15].

We reported the pH-dependent absorbance and fluorescent emission of some *Aequorea victoria*-derived FP and their use as indicators of organelle pH [16]. Swarup et al. [17] used this property to confirm the topology of the Aux1 auxin carrier in *Arabidopsis thaliana* root cells. The pH in the apoplastic space is approximately 5, and would cause complete quenching of the YFP tag; thus, the bright fluorescence of an N-YFP-Aux1 fusion indicated cytoplasmic localization of the Aux1 N-terminus.

Here we describe a simple PEA to ascertain membrane protein topology in living cells. By selectively modifying pH at either side of the PM, FPs fused to PM proteins show a pH-dependent change in fluorescence, indicating the extracellular/cytosolic orientation of the domain into which the FP was inserted. Use of PEA helped to establish that sst5c locates in the plasma membrane with a four-TM domain configuration and an extracellular C-terminus. In contrast to the methods described above, PEA allows quantification of the relative proportion of extracellular/cytosolic orientation for proteins with multiple topological forms. Comparative analysis of PrP^C with PEA thus demonstrated the existence of the elusive NtmPrP form in living cells and that this form reaches the plasma membrane.

Materials and methods

Reagents

We purchased 2′,7′-bis-(2-caboxyethyl)-5-(and-6)-carboxyfluorescein, acetoxymethyl ester (BCECF-AM) from Molecular Probes and Lipofectamine 2000 from Invitrogen. Nigericin, monensin and carbonyl cyanide *p*-(trifluoromethoxy) phenylhydrazone (FCCP) were from Sigma-Aldrich, and polyethylenimine was from Polysciences, Inc.

Plasmid constructs

GFP-TM was generated by cloning the regions encoding amino acid sequences 1–131 of human cytokine granulocyte-macrophage colony-stimulating factor and 239–272 of the human CD25 (IL-2-receptor alpha chain) into the *Nhe*I/*Hind*III and *Bsr*GI/*Xba*I sites, respectively, of the pEGFP-N1 vector (Clontech). YFP-TM was generated by substituting EYFP from pEYFP-N1 (Clontech) for EGFP in GFP-TM, using the *Hind*III/*Bsr*GI restriction sites. TM-YFP was produced by inserting the entire open reading frame of the chemokine receptor CXCR4 (a seven-transmembrane GPCR) into the multiple cloning site of pEYFP-N1 using *Hind*III and *Age*I sites [18, 19]. Acyl-GFP was generated by cloning the 12 N-terminal amino acid residues of human lymphocyte-specific protein tyrosine kinase (Lck) into the *Sac*I/*Kpn*I sites of pEGFP-N3. In Cit-acyl (previously termed mCit-HRASwt) [20], citrine, a YFP variant with a $pK_a = 5.7$ [21], was fused upstream of full-length Ha-Ras. The PrP-YFP plasmids encoding wtPrP-YFP and mutPrP-YFP (with mutations A2R-N3R-A120L) [10] were produced using multiple cloning steps to insert the N-terminal 1-223 and the C-terminal 220–254 amino acid regions of SHaPrP (Syrian hamster prion protein) into the *Nhe*I/*Age*I and the *Bsp*E1/*Eco*RI target sites of pEYFP, respectively, then corrected for reading frames. For the somatostatin receptor sst5c-YFP plasmid, the sequence coding for human somatostatin receptor sst5TMD4 [7] was amplified by PCR to remove the TAA stop codon, and inserted N-terminally into the *Hind*III and *Bam*HI sites of YFP(F46L) [22]. The 81 N-terminal amino acids from human membrane-anchored galactosyltransferase were fused with EYFP in pcDNA3 mammalian expression vector (Invitrogen) to generate GT-EYFP [16]. $GPBP_{91}$-YFP was a kind gift of Dr. Juan Saus (CIPF, Valencia, Spain). GPBPΔ102, a cDNA encompassing the entire coding sequence of GPBP [23] and part of its 5′UTR open reading frame (starting in Ala102) [8], was amplified by PCR and inserted into the pEYFP-C1 multicloning site (Clontech), in-frame relative to EYFP. All constructs were verified by nucleotide sequencing.

Cell culture and transfection

Cells were cultured in DMEM (HeLa and Be2C) or F-12 (CHO-K1) supplemented with heat-inactivated 10% FBS (fetal bovine serum; Cambrex Bioscience), 2 mM L-glutamine and penicillin/streptomycin (100 U/ml) (Cambrex) at 37°C with 5% CO_2. Cells were plated on coverslips (24 h), then transfected with 1 μg plasmid DNA and 2 μl Lipofectamine 2000, and incubated (24–36 h). PrP-YFP were transfected with 3 μl polyethylenimine, as fluorescent fibers appeared on the coverslip when Lipofectamine 2000 was used. For image acquisition at 22°C, coverslips were transferred to an Attofluor microscopy chamber (Molecular Probes), and medium was replaced with Hanks' balanced salt solution (HBSS).

Buffers for extracellular pH exchange experiments

The HBSS used contained (in mM) 1.26 $CaCl_2$, 5.36 KCl, 0.44 KH_2PO_4, 0.5 $MgCl_2$, 0.4 $MgSO_4$, 4.16 $NaHCO_3$, 0.34 Na_2HPO_4, 137 NaCl, 5 glucose and 10 HEPES (HBSS pH 7.4) or MES (HBSS pH 6). In cells perfused with pH 6 extracellular solution, pH_i decreased by 0.1–0.2 pH units, as determined with the pH indicator BCECF (imaging details are provided in Supplementary Materials and Methods).

Buffers for intracellular pH exchange experiments

pH_i can be clamped to a value that is a function of the concentration ratio of permeant acid (A) and base (B) and of pH_o [24]:

$$pH_i = pH_o - 0.5 \log\{[A]/[B]\}$$

Null buffered saline solutions were: (1) $HBSS_{null}$ pH_i 7.4 contained (in mM) 1.26 $CaCl_2$, 5.36 KCl, 0.44 KH_2PO_4, 0.5 $MgCl_2$, 0.4 $MgSO_4$, 4.16 $NaHCO_3$, 0.34 Na_2HPO_4, 100.5 NaCl, 5 glucose, 10 PIPES, 5 butyric acid and 31.5 trimethylamine, (2) $HBSS_{null}$ pH_i 6.6 contained (in mM) 1.26 $CaCl_2$, 5.36 KCl, 0.44 KH_2PO_4, 0.5 $MgCl_2$, 0.4 $MgSO_4$, 4.16 $NaHCO_3$, 0.34 Na_2HPO_4, 100.5 NaCl, 5 glucose, 10 PIPES, 31.5 butyric acid and 5 trimethylamine, and (3) $HBSS_{control}$ pH_o 7 contained (in mM) 1.26 $CaCl_2$, 5.36 KCl, 0.44 KH_2PO_4, 0.5 $MgCl_2$, 0.4 $MgSO_4$, 4.16 $NaHCO_3$, 0.34 Na_2HPO_4, 100.5 NaCl, 5 glucose, 10 PIPES and 36.5 Na^+-D-gluconate (to substitute for chloride). These buffers for intracellular pH exchange were adjusted to pH 7. Some caution must be taken when using null buffers with membrane-anchored YFP. Control and null buffers used here contained the same chloride concentration to avoid potential artifacts derived from the halide sensitivity of YFP [25], which is not shared by GFP, citrine [21] or Venus [26]. We loaded cells with the pH indicator BCECF to verify that null buffers changed pH_i (Fig. S1).

Cell superfusion

To exchange solutions completely from the cell chamber during imaging experiments, we used a saline superfusion system; input was driven by gravity, and output was obtained by suction from a fishtank pump (inverted flow).

Imaging setup

An epifluorescence inverted microscope (DMIRE-2, Leica) with a N.A. 1.25 40× oil immersion objective, and a polychromator (C7773, Hamamatsu) for excitation (500 nm) were used [27]. FP construct-transfected cells were imaged with filtercube BrightLine HC-YFP (Semrock 500/24 nm exciter, 520 nm dichroic and a 542/27 nm emitter, center wavelength/bandwidth). The detector was an electron-multiplying CCD (EMC9100-13, Hamamatsu). The polychromator and camera were controlled and images were acquired using AquaCosmos 2.6 software (Hamamatsu). Regions of interest (ROI) were selected manually on areas of cytoplasm or cell membrane. Pixel intensities were averaged spatially and corrected for background.

Orientation quantification

The topology standards for 100% cytoplasmic (TM-YFP) and 100% extracellular (YFP-TM) orientation showed fluorescence reductions of 10% and 82% after pH_o exchange, respectively (Fig. 1e). The fluorescence intensity reduction with pH_o exchange for each protein under study can be converted to % inside/outside topology by comparison with the quenching observed for these standards in our setup, as follows:

$$\text{Extracellular } (\%) = \left[\text{Quench}_{\text{pH}_o 6}(\%) - 10\right] \times 100/72$$

Statistical analysis

Error bars represent SD of the mean. Student's *t* test was used to evaluate the statistical significance of the changes.

Results

Design and construction of topology standards: integral and membrane-associated proteins

To obtain a battery of PM-targeted pH-sensitive FPs with varying extracellular/cytoplasmic (or organelle lumen/cytoplasmic) locations, we designed several constructs containing GFP (pK_a near 6), YFP (pK_a 7.1) or its mutant citrine (pK_a 5.7) fused to sequences encoding signal peptides, TM segments or membrane-anchoring motifs (Fig. 1a). As a model of a single-spanning TM protein with an extracellular FP (GFP-TM and YFP-TM), we designed a fusion protein containing residues 1–131 of granulocyte-macrophage colony-stimulating factor (with the signal sequence), followed by GFP/YFP and the CD25 238–272 sequence (including its TM region).

To model the cytosolic topology of the tag, we used TM-YFP, which consists of the fusion of EYFP and CXCR4, a chemokine receptor with seven TM domains and a cytoplasmic C-terminus. In acyl-GFP, the FP was fused C-terminally to Lck residues 1–12, which bear the acylation motifs for PM attachment at the cytoplasmic side. Citrine-acyl consists of the YFP variant citrine fused to Ha-Ras [20].

As a model for FP location at the Golgi lumen, we used GT-YFP, composed of the 1–81 N-terminal region of galactosyltransferase (containing the single TM domain and the Golgi targeting signal) and followed by the EYFP sequence [16]. We also included EYFP, a freely diffusible intracellular protein, as a control. These models were transiently expressed in HeLa cells and representative fluorescence images recorded (Fig. 1b). GFP-TM, YFP-TM, TM-YFP, acyl-GFP and citrine-acyl were observed abundantly on the PM, particularly at cell-cell contact areas.

Topology standards of membrane proteins and site-specific pH exchange: modifying extracellular, cytosolic or organelle pH

To verify the applicability of this method, we selectively modified extracellular or cytosolic pH in cells expressing the standards described (Fig. 1a, b). Change in extracellular pH (pH_o) would exclusively affect emission by FP facing the extracellular medium, whereas altering intracellular pH (pH_i) would only be sensed by FP facing the cytoplasm. The extent of fluorescence change would depend on the pK_a of the FP. As predicted, the fluorescence intensity of GFP-TM in the ROI on the PM decreased after cell perfusion with extracellular solution at pH 6 (HBSS pH 6) (Fig. 1c, top). For YFP-TM, HBSS pH 6 led to a greater fluorescence decrease (Fig. 1c, middle), consistent with its pK_a value of 7. Fluorescence decreased only slightly on the PM of TM-YFP-expressing cells superfused with HBSS pH 6 (Fig. 1c, bottom), compatible with cytoplasmic tag orientation.

To modify intracellular pH without extracellular change, we used the null buffer method [24, 28]. pH_i can be clamped using a mixture of permeant weak acid and base, while extracellular medium is maintained at physiological pH. After cell perfusion with low pH $HBSS_{null}$, the fluorescence intensity of GFP-TM and YFP-TM on the PM was almost unaltered, confirming the extracellular orientation of these tags (Fig. 1d, top and middle); in contrast, TM-YFP emission decreased with the same pH manipulation (intracellular tag).

We correlated the fluorescence quench of the standards with their predicted orientation (and pK_a) following change in pH_o and pH_i (Fig. 1e). Lowering pH_o from 7.4 to 6 produced <10% change in membrane fluorescence of

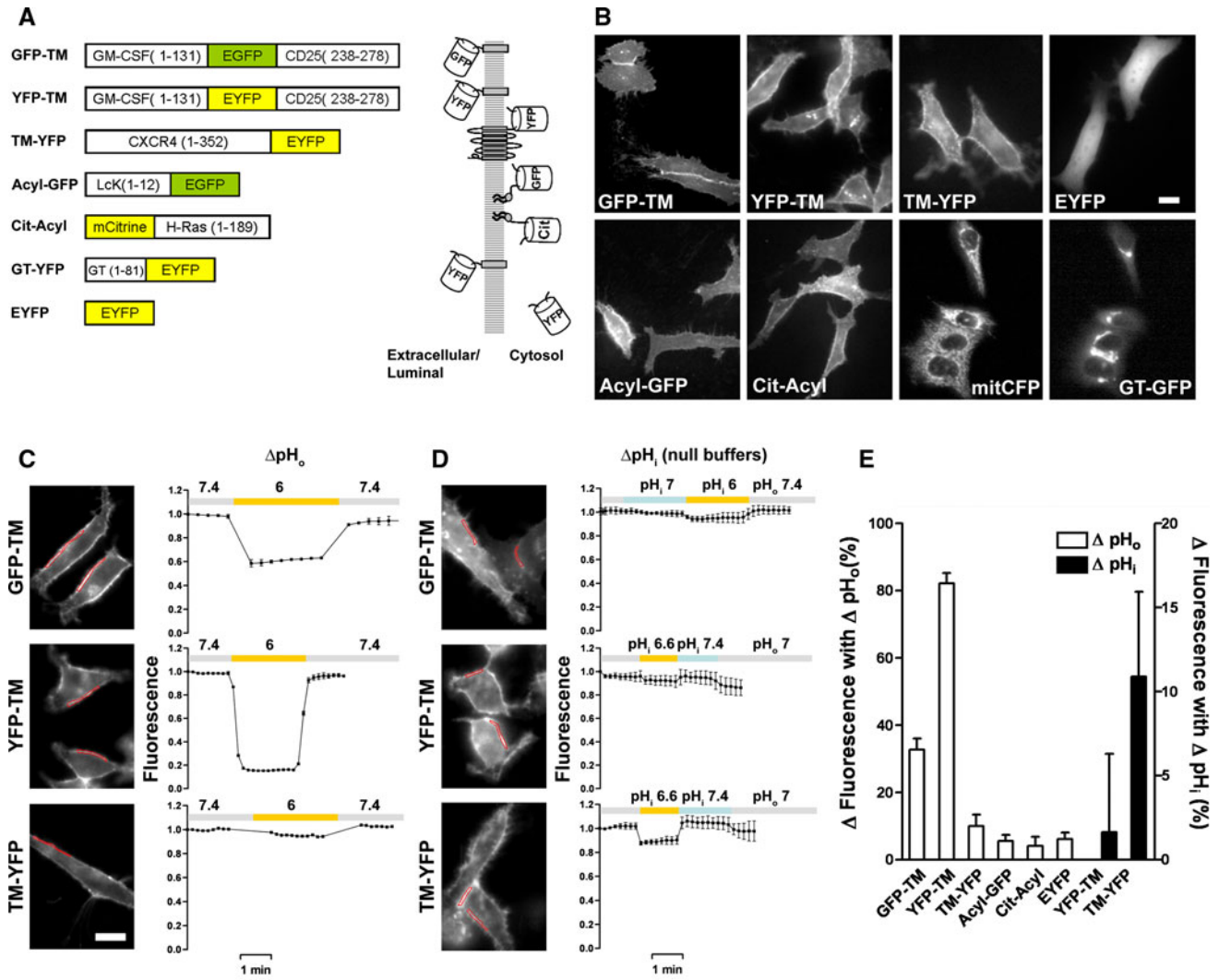

Fig. 1 Fluorescent protein topology standards with their predicted membrane orientations. **a** Construct scheme, nomenclature and predicted membrane orientation of the topology standards. **b** Representative fluorescence images of HeLa cells expressing topology standards. The cells (*bottom right*) were cotransfected with GT-YFP and mitochondrially targeted CFP (mitCFP). **c**, **d** PEA to determine the orientation of membrane protein fluorescent tags. Fluorescence images of living cells used in representative extracellular (pH_o; **c**) or intracellular (pH_i; **d**) PEA experiments. ROI for intensity quantification on the PM are shown in *red*. The time course for average intensity during perfusion with the indicated buffer is shown. **e** Percent fluorescence decrease of topology standard proteins after change in pH_o (*open bars*) or pH_i (*filled bars*) (note scale difference). pH_o change was from 7.4 to 6; pH_i change was from 7.4 to 6.6. Acidification of extracellular buffer provides a more sensitive readout of topology than pH_i change. *Scale bars* 10 μm

fusion proteins designed for cytoplasmic FP orientation (acyl-GFP, Cit-acyl, TM-YFP). Cytoplasmic, freely diffusible EYFP decreased 6% in pH_o 6 buffer. Intracellular pH is maintained constant by the action of many mechanisms, but we observed that $pH_o = 6$ causes a pH_i decrease of 0.1–0.2 (measured by BCECF), which is sensed by cytoplasm-oriented FP. In contrast, YFP-TM decreased by 82% after pH_o exchange from 7.4 to 6 (Fig. 1e). As predicted by pK_a values, GFP-TM fluorescence decreased less (33% drop) than YFP-TM; the qualitative result is nonetheless the same, regardless of the FP variant used. These results were mirrored when pH_i was decreased with null buffers; TM-YFP fluorescence decreased by 11%, and YFP-TM was unaffected (2% drop). The fluorescence decrease was greater with pH_o than with pH_i exchange, and null buffers should thus be used only to confirm pH_o results.

We used the PEA to analyze the topology of intracellular membrane-associated proteins in organelles with a pH gradient across the membrane. The secretory pathway downstream of the ER is progressively acidified, as are endosomes/lysosomes, whereas the mitochondrial matrix is

alkaline with respect to cytosol. Organellar pH can be manipulated in live cells; inhibitors of the V-type proton ATPase cancel out the pH gradient of the Golgi by H^+ diffusion [29], and protonophores disrupt the H^+ gradient across all membranes [16]. GT-YFP-transfected HeLa cells show Golgi staining (Fig. 1b), and fluorescence over Golgi ROI doubled within 1 min of FCCP protonophore application (Fig. 2e), confirming localization at the Golgi lumen [16].

Distinguishing between alternative predicted topologies of a short somatostatin receptor splice variant

Having demonstrated the method with standards of known orientation, we used it to distinguish between alternative predicted topologies of a truncated isoform of sst5. Canonical GPCRs have a well-conserved topology consisting of an extracellular N-terminal domain, seven TM regions and an intracellular C-terminus involved in signal transduction and desensitization [30]. For a specific splice variant of human sst5 (sst5c), the hydrophobicity profile obtained using different algorithms predicted either three or four membrane-spanning segments, implying alternative location of the C-terminus. For GPCR, tagging with FP has been widely used in the study of dynamic processes, such as interaction to form homo- and heterodimers, internalization or binding affinity. We generated a C-terminal YFP fusion of sst5c (Fig. 2a). CHO-K1 cells transfected with the expression vector showed mostly intracellular fluorescence, with some PM staining (Fig. 2a) [7]. This

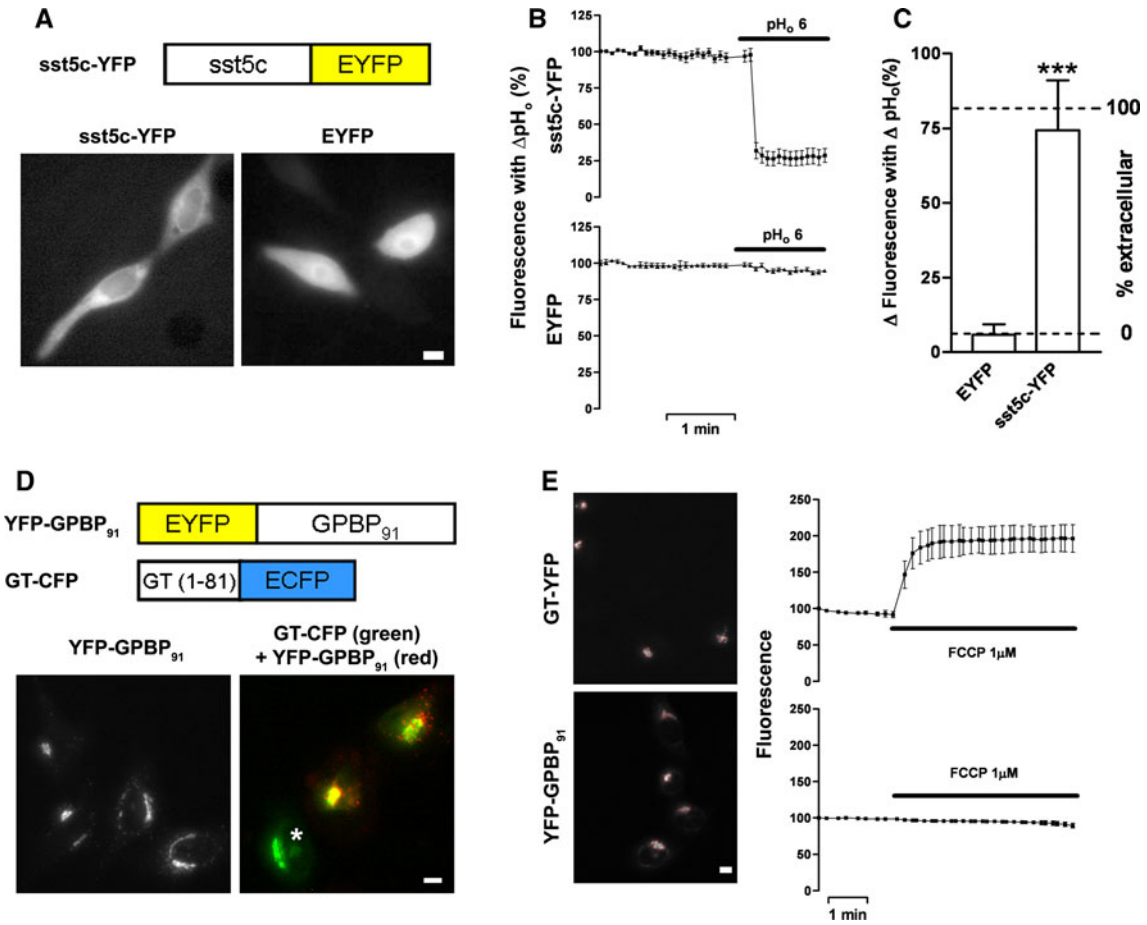

Fig. 2 Application of PEA to assess topology of membrane proteins with unknown orientation: the truncated somatostatin receptor sst5c (**a**–**c**) and protein kinase $GPBP_{91}$ (**d**, **e**). **a** Construct scheme and fluorescence images of live CHO-K1 cells expressing sst5c-YFP or control cytoplasmic EYFP. **b** Time course of average fluorescence intensity in PM ROI of either sst5c-YFP or EYFP transfected cells during cell superfusion from pH_o 7.4 to 6. **c** Analysis of sst5c-YFP orientation by quantifying fluorescence decrease (%) and comparison with controls EYFP and YFP-TM (*dotted lines*). For sst5c-YFP versus EYFP, $***P < 0.0001$. **d** YFP-$GPBP_{91}$ and GT-CFP construct scheme. Fluorescence of YFP-$GPBP_{91}$-transfected HeLa cells shows Golgi staining plus some punctate labeling (*left*). Cotransfection of YFP-$GPBP_{91}$ plus the Golgi-targeted GT-CFP (*right*). YFP-$GPBP_{91}$ is coded in *red* and GT-CFP in *green*. The perinuclear fluorescence of YFP-$GPBP_{91}$, but not its punctate staining, colocalized (*yellow*) with GT-CFP. One cell (*) expressed GT-CFP alone. **e** Fluorescence image and average intensity over the Golgi region in GT-YFP- or YFP-$GPBP_{91}$-expressing cells during addition of 1 μM FCCP. GT-YFP, but not YFP-$GPBP_{91}$ was sensitive to the FCCP-induced increase in lumenal pH, indicating that YFP is lumenal only in GT-YFP-expressing cells. *Scale bars* 10 μm

subcellular localization was similar to that found for the endogenous receptor in paraffin sections of human pituitary tumors, as was determined by immunochemistry [7]. Acidification of the extracellular medium quenched 75% of initial sst5c-YFP fluorescence at the PM (Fig. 2c), whereas intensity of cells transfected with cytoplasmic EYFP was reduced by 7% (Fig. 2b, c), comparable to a 10% decrease of cytoplasmic tag TM-EYFP (Fig. 1e). Thus, sst5c-YFP present at the plasma membrane has the C-terminal YFP tag 100% extracellular. This sst5 variant is a 4-TM domain receptor with an extracellularly oriented C-terminus and is henceforth referred to as sst5TMD4. We have not investigated sst5c receptor found intracellularly.

Localization of the N-terminus of a protein associated to Golgi membranes ($GPBP_{91}$)

Alternate translation initiation can also change the membrane interaction properties of some gene products, as is the case of $GPBP_{91}$, a 91-kDa intracellular variant of the extracellular Ser/Thr kinase Goodpasture antigen-binding protein (GPBP) [8, 23]. This variant was YFP-tagged (YFP-$GPBP_{91}$) to define its topology (Fig. 2d). YFP-$GPBP_{91}$-transfected HeLa cells showed perinuclear staining, as well as punctate staining that extended from the nucleus (Fig. 2d). The perinuclear labeling colocalized with the cyan version of GT-YFP, as shown in cotransfection experiments, and thus corresponds to Golgi apparatus. Fluorescence intensity on Golgi ROI in YFP-$GPBP_{91}$-expressing cells remained unchanged after application of the protonophore FCCP, in contrast to results with the Golgi luminal standard GT-YFP (Fig. 2e). YFP-$GPBP_{91}$ is thus Golgi-associated in HeLa cells, and its N-terminus resides on the cytoplasmic side of Golgi membranes. This result also serves as proof of concept of intracellular membrane topology assignment by PEA in acidic organelles.

Distinction between two isoforms of a protein: SecPrP and NtmPrP

In addition to mechanisms that modify the covalent structure of the polypeptide chain, its interaction with the translocon components can also alter final topology. Proteins displaying multiple topologic forms arising from the same mRNA will thus elude computational prediction programs [3]. Biogenesis studies of the cellular prion protein (PrP^{C}) (structure shown in Fig. 3a) show that it can adopt three membrane-bound conformations: a glycosylphosphatidylinositol (GPI)-anchored form resulting from full translocation in the ER (SecPrP) and two membrane-integrated forms with opposite orientation (NtmPrP, with a cytosolic C-terminus, and CtmPrP, with a cytosolic N-terminus) [31] (Fig. 3b). We constructed the fusion proteins wtPrP-YFP and mutPrP-YFP (containing the A2R-N3R-A120L mutations, previously shown to favor the NtmPrP conformation in in vitro biochemical assays) [10] by inserting the tag between the C-terminal globular domain and the signal for GPI addition (Fig. 3a). This insertion site yields a fusion product that undergoes normal maturation and processing and behaves as a dominant-negative inhibitor that binds to the infectious conformer PrP^{Sc} [32–34]. The wild-type (wt) chain is predicted to yield predominantly SecPrP (extracellular YFP), whereas mutPrP would be enriched in NtmPrP (cytoplasmic YFP) [10] (Fig. 3b). Both proteins showed abundant PM labeling with some intracellular punctate and occasional perinuclear, Golgi-like staining (Fig. 3c). Decreasing pH_o from 7.4 to 6.0 reduced PM fluorescence by 71 and 64% for wtPrP-YFP and mutPrP-YFP, respectively (Fig. 3d). This distribution was confirmed in human Be(2)C neuroblastoma cells (Fig. S2). The topology standards for 100% inside (TM-YFP) and 100% outside (YFP-TM) orientation showed fluorescence reductions of 10 and 82% after pH_o exchange, respectively. Comparison of these values with fluorescence change for PrP variants showed that the C-terminus of wtPrP-YFP and mutPrP-YFP are 85 and 75% extracellular, respectively (Fig. 3e), in accordance with data from pH_i change using null buffers (Fig. 3d). The A2R-N3R-A120L mutations thus led to 10% higher NtmPrP expression at the PM compared to the wtPrP sequence in live HeLa cells. These results also confirm the existence of the NtmPrP form in cells and show its distribution at the plasma membrane.

Discussion

Several approaches that address membrane protein topology in living systems rely on constructing fusion proteins with FP and have been used to clarify inconclusive topology predictions obtained by computational methods. The *Arabidopsis thaliana* ER retention receptor ERD2 has seven hydrophobic domains in its primary sequence and algorithms predicted from none to seven TM domains [15]. Although seven TM domains were proposed for the human ERD2.1 and *S. cerevisiae* K/HDEL receptors, experimental validation with a redox-based topology assay demonstrated that *A. thaliana* ERD2 has six TM domains. The *A. thaliana* auxin permease Aux1 was likewise predicted to have from 7 to 11 TM domains, with a consensus of 10 TM domains using the ARAMEMNON database [17]. pH sensitivity studies using YFP-tagged Aux1 nonetheless demonstrated that the first hydrophobic region spanned the membrane not once, but twice, and that Aux1 therefore has 11 TM domains. In this case, prediction programs failed because of the close proximity of the first two TM regions, separated only by a single amino acid residue. These

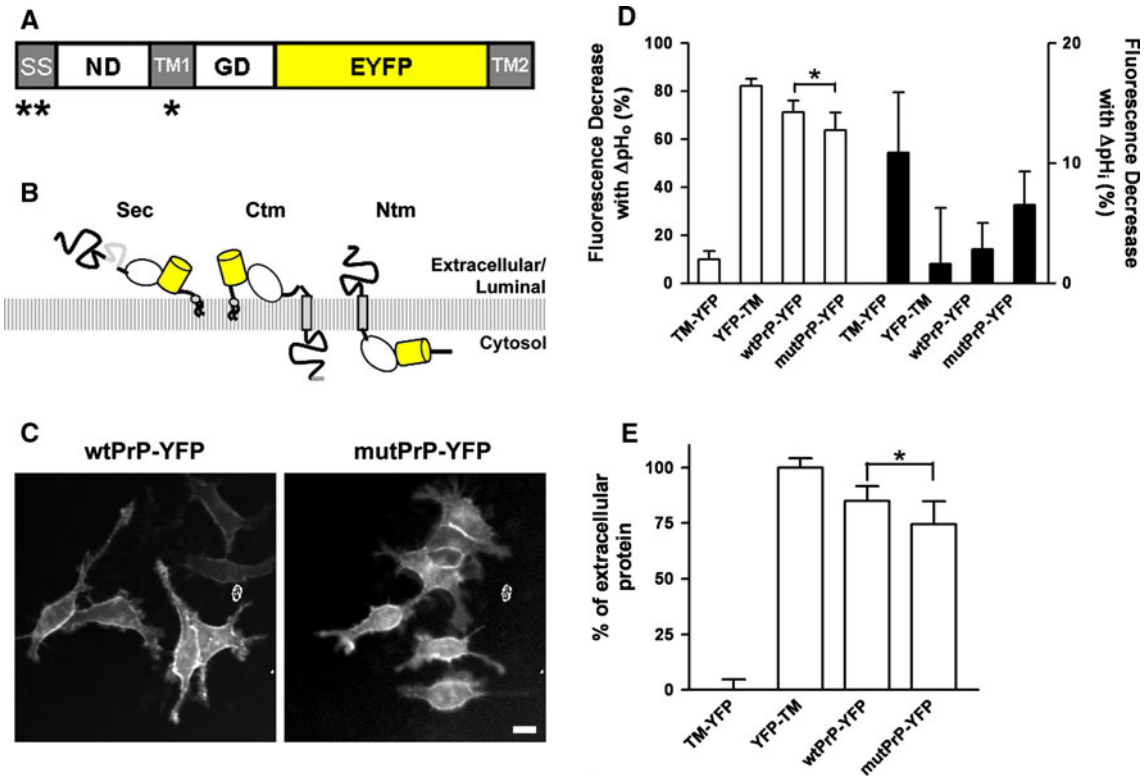

Fig. 3 Determination of cellular prion protein (PrP^C) topology in living cells. **a** EYFP-labeled chimeric PrP^C, showing the relative position of domains. *SS* signal sequence, *ND* N-terminal domain, *GD* globular domain. *Asterisks* mark point mutations in mutPrP **b** Scheme showing possible PrP-YFP topologies: SecPrP-YFP, CtmPrP-YFP and NtmPrP-YFP. **c** Fluorescence of HeLa cells expressing wtPrP-YFP or mutPrP-YFP (bearing point mutations A2R, N3R and A120L) [10]. **d** Fluorescence decrease of PrP constructs induced by pH_o (7.4–6, *open bars*) or pH_i exchange (7.4–6.6, *filled bars*) compared to topology standards TM-YFP (intracellular tag) and YFP-TM (extracellular tag). **e** Using TM-YFP and YFP-TM standard values as 100% intra- or extracellular, respectively, the proportion was estimated for PrP forms with a cytoplasmic or an extracellular C-terminus. $*P = 0.0167$. *Scale bar* 20 μm

examples reinforce the need to experimentally confirm topology conclusions obtained with other methods.

We propose a method to verify the topology of PM integral proteins with one or more putative TM domains, membrane-associated proteins and compartmentalized proteins of acidic/alkaline organelles in living cells. As proof of concept, we constructed cytoplasmic and extracellular topology standards based on well-characterized PM proteins. We studied three proteins that pose problems commonly encountered in topology assignment. First, a truncated GPCR generated by splicing of cryptic introns at the sst5 mRNA [7] was shown to have four TM domains (sst5TMD4) and a C-terminus that cannot participate in signaling to G proteins because it is extracellular, at difference from canonical seven-TM GPCR. Ascertaining the topology of these domains is essential before functional characterization of a novel receptor, first because it defines its putative ligand-binding pocket using homology modeling and second because it gives some information about downstream signaling pathways [35]. Clarification of structure-function relationships in these GPCR with less than seven TM domains is of pathophysiological importance, because of their appearance in pituitary tumors and their intriguing ligand sensitivity [7].

The canonical 77-kDa GPBP has been observed as a soluble protein in the extracellular medium, where its phosphorylation target (a domain in type IV collagen) is found [8, 23]; both $GPBP/CERT_L$ and its splice variant GPBPΔ26/CERT are cytosolic non-vesicular ceramide transporters between the ER, its synthesis site, to the Golgi apparatus, where it is converted to sphingomyelin [36]. In addition to these forms, 91-kDa $GPBP_{91}$ was recently proposed to arise by non-canonical translation initiation, and it was not detected in the soluble fraction, but in mitochondrial/lysosomal and microsomal fractions [8]. We found $YFP\text{-}GPBP_{91}$ to be Golgi-associated, and PEA analysis revealed that its N-terminus (the YFP-tagged domain) was cytoplasmic. It is conceivable that YFP tagging or enhanced expression interfered with correct targeting or topology of $GPBP_{91}$; nevertheless, our data are consistent with GPBP function in ceramide transport from the ER to Golgi [36], and with the finding that $GPBP_{91}$ is membrane-associated [8].

Our third example was PrP^C. Although it is viewed as a single protein, it is indeed a family of proteins derived from a single mRNA that differ in their capacity to segregate outside and inside the secretory route and in their membrane binding mode [9–12]. Of these, NtmPrP is a transmembrane form observed in cell-free systems that recalls a translocation-stalled intermediate [10], but whose presence in cells was unknown. PEA analysis of wtPrP and mutPrP (bearing mutations shown in vitro to favor the NtmPrP conformation) identified differences that support the existence of the NtmPrP form in cells and its location at the PM. These findings will help to elucidate PrP^C functions such as interpretation of proteolytic post-translational processing (α-/β-cleavage), as well as adaptor molecules involved in the related signal transduction and availability of C-terminal domains for PrP^C conversion into PrP^{Sc} [31].

What are the advantages of PEA over other methods for establishing membrane protein topology? It employs the widely used *Aequorea*-derived GFP or YFP (or other pH-sensitive variants). In contrast, both bimolecular fluorescence complementation [14] and redox-based topology assays [15] require very specific FPs (split YFP and roGFP, respectively). PEA does not require potentially deleterious treatments such as cell permeabilization or proteolysis. The fluorescent protease protection assay [13] depends on fine adjustment of digitonin concentration for sufficient PM permeabilization, while preventing perforation of intracellular membranes. In PEA, fluorescence intensity is measured in small ROIs, so it might be affected by cell movement or defocusing upon pH exchange during imaging. This was avoided by doing short time courses (3–5 min, Figs. 1, 2, 3) and by using a gravity-driven perfusion system that eliminates vibrations. Ratiometric imaging is less influenced by cell movement, so PEA could easily be adapted by using the pH sensor ratiometric pHluorin [37]. PEA could also be used to test the membrane orientation of multiple-TM domain proteins by their successive deletion, as reported for ERD2 with the redox-based topology assay [15], or by stepwise insertion of a YFP tag in each of the putative loops between TM domains.

The PEA is a minimally invasive method with which to verify protein topology in living cells, provides binary (in/out) information and can indicate the percentage of each topology for proteins with multiple orientations, as shown here for PrP^C. Production of the FP fusions is straightforward; as hundreds of functional fusions with GFP or YFP variants are available, the assay is immediately applicable for confirmation or disclosure of the topology of a large number of membrane proteins.

Acknowledgments The authors thank Dr. Juan Saus for the gift of reagents and helpful discussions on GPBP biochemistry and C. Mark for editorial assistance. BD was supported by FISCAM (MOV-2006_IE/07), MD-P by MICINN (Sara Borrell Program CD07/00246) and TF by MICINN (Ramón y Cajal contract). This work was supported by grants from the Spanish Ministry of Science and Innovation MICINN/FEDER BFU2008-03288 (JL), SAF2006-00418 and BFU2009-07971 (MG), BFU2007-60180 (JPC), the Junta de Andalucía BIO-0139 and CTS-01705 (JPC), European Union MRTN-2005-019481 (JL) and MIRG-CT-2006-026702 (TF) and Instituto de Salud Carlos-III FIS-PI052270 (TF).

Conflict of interest statement MD-P and JPC are listed as the inventors of patent PCT/ES2007/00627 for the commercial use of sst5TMD4. The remaining co-authors declare no conflict of interest.

References

1. Ahram M, Litou ZI, Fang R, Al-Tawallbeh G (2006) Estimation of membrane proteins in the human proteome. In Silico Biol 6(5):379–386
2. Elofsson A, von Heijne G (2007) Membrane protein structure: prediction versus reality. Annu Rev Biochem 76:125–140
3. Ott CM, Lingappa VR (2002) Integral membrane protein biosynthesis: why topology is hard to predict. J Cell Sci 115:2003–2009
4. McWilliams DF, Watson SA, Crosbee DM, Michaeli D, Seth R (1998) Coexpression of gastrin and gastrin receptors (CCK-B and delta CCK-B) in gastrointestinal tumour cell lines. Gut 42:795–798
5. Rekasi Z, Czompoly T, Schally AV, Halmos G (2000) Isolation and sequencing of cDNAs for splice variants of growth hormone-releasing hormone receptors from human cancers. Proc Natl Acad Sci USA 97:10561–10566
6. Havt A, Schally AV, Halmos G, Varga JL, Toller GL, Horvath JE, Szepeshazi K, Koster F, Kovitz K, Groot K, Zarandi M, Kanashiro CA (2005) The expression of the pituitary growth hormone-releasing hormone receptor and its splice variants in normal and neoplastic human tissues. Proc Natl Acad Sci USA 102:17424–17429
7. Duran-Prado M, Gahete MD, Martinez-Fuentes AJ, Luque RM, Quintero A, Webb SM, Benito-Lopez P, Leal A, Schulz S, Gracia-Navarro F, Malagon MM, Castano JP (2009) Identification and characterization of two novel truncated but functional isoforms of the somatostatin receptor subtype 5 differentially present in pituitary tumors. J Clin Endocrinol Metab 94:2634–2643
8. Revert F, Ventura I, Martinez-Martinez P, Granero-Molto F, Revert-Ros F, Macias J, Saus J (2008) Goodpasture antigen-binding protein is a soluble exportable protein that interacts with type IV collagen. Identification of novel membrane-bound isoforms. J Biol Chem 283:30246–30255
9. Juanes ME, Elvira G, Garcia-Grande A, Calero M, Gasset M (2009) Biosynthesis of prion protein nucleocytoplasmic isoforms by alternative initiation of translation. J Biol Chem 284:2787–2794
10. Kim SJ, Rahbar R, Hegde RS (2001) Combinatorial control of prion protein biogenesis by the signal sequence and transmembrane domain. J Biol Chem 276:26132–26140
11. Levine CG, Mitra D, Sharma A, Smith CL, Hegde RS (2005) The efficiency of protein compartmentalization into the secretory pathway. Mol Biol Cell 16:279–291
12. Rane NS, Yonkovich JL, Hegde RS (2004) Protection from cytosolic prion protein toxicity by modulation of protein translocation. EMBO J 23:4550–4559

13. Lorenz H, Hailey DW, Lippincott-Schwartz J (2006) Fluorescence protease protection of GFP chimeras to reveal protein topology and subcellular localization. Nat Methods 3:205–210
14. Zamyatnin AA Jr, Solovyev AG, Bozhkov PV, Valkonen JP, Morozov SY, Savenkov EI (2006) Assessment of the integral membrane protein topology in living cells. Plant J 46:145–154
15. Brach T, Soyk S, Muller C, Hinz G, Hell R, Brandizzi F, Meyer AJ (2009) Non-invasive topology analysis of membrane proteins in the secretory pathway. Plant J 57:534–541
16. Llopis J, McCaffery JM, Miyawaki A, Farquhar MG, Tsien RY (1998) Measurement of cytosolic, mitochondrial, and Golgi pH in single living cells with green fluorescent proteins. Proc Natl Acad Sci USA 95:6803–6808
17. Swarup R, Kargul J, Marchant A, Zadik D, Rahman A, Mills R, Yemm A, May S, Williams L, Millner P, Tsurumi S, Moore I, Napier R, Kerr ID, Bennett MJ (2004) Structure-function analysis of the presumptive Arabidopsis auxin permease AUX1. Plant Cell 16:3069–3083
18. Mellado M, Serrano A, Martinez C, Rodriguez-Frade JM (2006) G protein-coupled receptor dimerization and signaling. Methods Mol Biol 332:141–157
19. Pello OM, Martinez-Munoz L, Parrillas V, Serrano A, Rodriguez-Frade JM, Toro MJ, Lucas P, Monterrubio M, Martinez A, Mellado M (2008) Ligand stabilization of CXCR4/delta-opioid receptor heterodimers reveals a mechanism for immune response regulation. Eur J Immunol 38:537–549
20. Peyker A, Rocks O, Bastiaens PI (2005) Imaging activation of two Ras isoforms simultaneously in a single cell. Chembiochem 6:78–85
21. Griesbeck O, Baird GS, Campbell RE, Zacharias DA, Tsien RY (2001) Reducing the environmental sensitivity of yellow fluorescent protein. Mechanism and applications. J Biol Chem 276:29188–29194
22. Duran-Prado M, Bucharles C, Gonzalez BJ, Vazquez-Martinez R, Martinez-Fuentes AJ, Garcia-Navarro S, Rhodes SJ, Vaudry H, Malagon MM, Castano JP (2007) Porcine somatostatin receptor 2 displays typical pharmacological sst2 features but unique dynamics of homodimerization and internalization. Endocrinology 148:411–421
23. Raya A, Revert F, Navarro S, Saus J (1999) Characterization of a novel type of serine/threonine kinase that specifically phosphorylates the human goodpasture antigen. J Biol Chem 274:12642–12649
24. Eisner DA, Kenning NA, O'Neill SC, Pocock G, Richards CD, Valdeolmillos M (1989) A novel method for absolute calibration of intracellular pH indicators. Pflugers Arch 413:553–558
25. Wachter RM, Remington SJ (1999) Sensitivity of the yellow variant of green fluorescent protein to halides and nitrate. Curr Biol 9:R628–R629
26. Nagai T, Ibata K, Park ES, Kubota M, Mikoshiba K, Miyawaki A (2002) A variant of yellow fluorescent protein with fast and efficient maturation for cell-biological applications. Nat Biotechnol 20:87–90
27. Domingo B, Sabariegos R, Picazo F, Llopis J (2007) Imaging FRET standards by steady-state fluorescence and lifetime methods. Microsc Res Tech 70:1010–1021
28. Szatkowski MS, Thomas RC (1986) New method for calculating pHi from accurately measured changes in pHi induced by a weak acid and base. Pflugers Arch 407:59–63
29. Wu MM, Llopis J, Adams SR, McCaffery JM, Teter K, Kulomaa MS, Machen TE, Moore HP, Tsien RY (2000) Studying organelle physiology with fusion protein-targeted avidin and fluorescent biotin conjugates. Methods Enzymol 327:546–564
30. Kristiansen K (2004) Molecular mechanisms of ligand binding, signaling, and regulation within the superfamily of G-protein-coupled receptors: molecular modeling and mutagenesis approaches to receptor structure and function. Pharmacol Ther 103:21–80
31. Aguzzi A, Baumann F, Bremer J (2008) The prion's elusive reason for being. Annu Rev Neurosci 31:439–477
32. Barmada SJ, Harris DA (2005) Visualization of prion infection in transgenic mice expressing green fluorescent protein-tagged prion protein. J Neurosci 25:5824–5832
33. Hachiya NS, Watanabe K, Sakasegawa Y, Kaneko K (2004) Microtubules-associated intracellular localization of the NH2-terminal cellular prion protein fragment. Biochem Biophys Res Commun 313:818–823
34. Medrano AZ, Barmada SJ, Biasini E, Harris DA (2008) GFP-tagged mutant prion protein forms intra-axonal aggregates in transgenic mice. Neurobiol Dis 31:20–32
35. Lundin C, Kall L, Kreher SA, Kapp K, Sonnhammer EL, Carlson JR, Heijne G, Nilsson I (2007) Membrane topology of the Drosophila OR83b odorant receptor. FEBS Lett 581:5601–5604
36. Hanada K, Kumagai K, Yasuda S, Miura Y, Kawano M, Fukasawa M, Nishijima M (2003) Molecular machinery for non-vesicular trafficking of ceramide. Nature 426:803–809
37. Miesenbock G, De Angelis DA, Rothman JE (1998) Visualizing secretion and synaptic transmission with pH-sensitive green fluorescent proteins. Nature 394:192–195